ELECTRICAL EXPRESSION OF SPIN ACCUMULATION IN FERROMAGNET/SEMICONDUCTOR STRUCTURES

Łukasz Cywiński,* Hanan Dery†, Parin Dalal, and L. J. Sham
Department of Physics, University of California San Diego La Jolla, California 92093-0319, USA

We treat the spin injection and extraction via a ferromagnetic metal/semiconductor Schottky barrier as a quantum scattering problem. This enables the theory to explain a number of phenomena involving spin-dependent current through the Schottky barrier, especially the counter-intuitive spin polarization direction in the semiconductor due to current extraction seen in recent experiments. A possible explanation of this phenomenon involves taking into account the spin-dependent inelastic scattering via the bound states in the interface region. The quantum-mechanical treatment of spin transport through the interface is coupled with the semiclassical description of transport in the adjoining media, in which we take into account the in-plane spin diffusion along the interface in the planar geometry used in experiments. The theory forms the basis of the calculation of spin-dependent current flow in multi-terminal systems, consisting of a semiconductor channel with many ferromagnetic contacts attached, in which the spin accumulation created by spin injection/extraction can be efficiently sensed by electrical means. A three-terminal system can be used as a magnetic memory cell with the bit of information encoded in the magnetization of one of the contacts. Using five terminals we construct a reprogrammable logic gate, in which the logic inputs and the functionality are encoded in magnetizations of the four terminals, while the current out of the fifth one gives a result of the operation.

PACS numbers:

I. INTRODUCTION

Electrical spin injection (transfer of spin polarization by electrical current) from a ferromagnet into a paramagnet was first achieved in junctions between metals by Johnson and Silsbee.[1,2] The spin injection into semiconductors has proven to be a harder task.[3] In late 90s a successful spin injection at low temperatures from Mn-doped diluted ferromagnetic semiconductors[4,5,6,7] gave new impetus to the field of semiconductor spintronics. Injection from ferromagnetic metals at temperatures up to the room temperature followed soon afterwards.[8,9,10] Initially[8] the injection had quite low efficiency, which was was later increased,[9,11,12] with maximum reported[11] value of 30%. The rise in spin injection efficiency was achieved by a proper doping of the metal/semiconductor interface.[13,14,15] Spin extraction was also seen through optical measurement of spin accumulation in forward-biased MnAs/GaAs junction.[16]

During the last two years, there was a tremendous progress in both spin injection and extraction in Fe/GaAs structures. The spin accumulation due to both spin injection from Fe and spin extraction from GaAs into Fe (a depletion of spins which can move more easily into the magnet) were imaged by Kerr spectroscopy.[17] Soon afterwards the spin accumulation in the semiconductor near the junction with a magnet has been sensed electrically,[18,19] proving that the current through the metal/semiconductor junction depends on spin polarization of electrons inside the semiconductor.

In these experiments[17,18,19] an unexpected sign of spin accumulation near the drain was seen. For source and drain with parallel magnetizations, and for potential drops at the interfaces small compared to the energy scale on which the spin-projected densities of states in the ferromagnets change significantly, spins of opposite directions should accumulate near source and drain contacts. Contrary to this expectation, which is a consequence of time-reversal symmetry for elastic tunneling between the two materials,[20] the observed spin accumulation near the drain had the same sign as the one near the source contact. In Sec. II B we review a theory[21] of spin extraction which takes into account inelastic scattering through the bound states near the interface. These arise from the inhomogeneous profile of heavy n-type doping of the semiconductor near the junction with the metal.[13,14,15] This doping makes the Schottky barrier thin enough (∼10 nm) for efficient spin transport via tunneling. It also results in the creation of a potential well for electrons next to the barrier. At forward bias, the electrons from the bulk of the semiconductor either tunnel directly into the metal (elastic process), or scatter inelastically into the quasi-bound states in the well, and then leak out into the magnet. These two channels of electron transport through the interface favor opposite spin orientations, leading to opposite signs of spin accumulation. An alternative theory based on first-principles calculation of interface electronic structure (but neglecting the bending of the conduction band potential in GaAs) has also been proposed.[22]

Efficient spin injection/extraction is a basic prerequisite for any kind of practical application of spintronics systems. The simplest spintronics device is a two-

†Current address: Department of Electrical and Computer Engineering, University of Rochester, Rochester, NY 14627, USA

terminal spin valve, in which a current is passed between two ferromagnetic contacts connected through a paramagnetic channel. However, in electronics three-terminal semiconductor devices are indispensable for their switching (biasing the gate of a field effect transistor) or amplification capabilities (driving a current into the base of a bipolar transistor). Many types of "spin transistors" have been proposed theoretically. The most famous is the simple "current modulator" proposed by Datta and Das[23] in 1990, in which the electric field of the gate together with Rashba spin-orbit interaction[24,25] in the small-bandgap semiconductors controls the spin precession of ballistic electrons injected and extracted by ferromagnetic contacts. Despite a large experimental effort a conclusive demonstration of the device operation has remained elusive. Let us mention some of the other proposed semiconductor spin-transistors. A diffusive version of a Datta-Das system has been put forth.[26] Magnetic unipolar[27] and bipolar transistors[28,29,30] (both of which require non-degenerate magnetic semiconductors) have been analyzed. Another proposal was that of a spin transistor without any ferromagnetic elements,[31] which relies exclusively on strong spin-orbit interaction experienced by electrons in small bandgap materials such as InAs. There was also an idea of bypassing the problems with efficient spin injection and using a proximity effect of a ferromagnetic gate.[32,33] Here, we review our theoretical work on a class of systems consisting of a semiconductor channel with multiple ferromagnetic contacts attached. We work in the regime of diffusive spin transport at room temperature, and we concentrate on Fe/GaAs structures. However, we do not exploit strong spin-orbit interaction present in III-V semiconductors; the spin-orbit scattering serves only as a source of spin relaxation. Consequently, the proposed devices are also suited for silicon-based systems, as the spin relaxation time in Si is expected to be at least an order of magnitude longer than in GaAs. This makes silicon a perfect candidate for spintronics applications which do not rely on spin manipulation through spin-orbit interaction. The existence of spin-dependent coupling through a heavily doped Schottky junction between Si and a paramagnetic metal has been shown indirectly.[34] Recently, progress has been made[35] in creating tunneling contacts with widely tunable conductance between a ferromagnet and Si, albeit without showing yet spin injection. It is encouraging that hot electron spin injection into silicon accompanied by a magnetoresistive effect has been achieved recently,[36] as well as spin injection from iron into silicon using aluminum oxide tunneling barriers.[37]

Our review is organized as follows. In Sec. II we give a theory of spin-polarized transport through the heavily doped metal/semiconductor interface. Spin injection at large reverse bias is described in Sec. II A. For spin extraction we introduce in Sec. II B a new mechanism of spin transport through the junction due to leakage of localized electrons from the potential well close to the interface, and we show that it gives an opposite sign of spin accumulation to the mechanism of direct tunneling between the bulk of the semiconductor and the metal. Then in Sec. II C we consider a special case of an "optimally doped" barrier (without a pronounced potential well) kept at low bias, which can be used as an electrical probe of the spin accumulation in the semiconductor. In Sec. III we couple the description of spin injection/extraction with the diffusive transport inside the semiconductor, and we explain the significance of spin accumulation for magnetoresistance of a two-terminal system (a spin valve). We introduce the basic concept of electrical sensing of the spin splitting in the semiconductor using a ferromagnetic contact in Sec. IV. The possible applications, including the Magnetic Contact Transistor[38] and a magneto-logic gate integrable into a large-scale circuit[39] are presented in Sec. IV and are illustrated by theoretical calculations.

II. SPIN TRANSPORT THROUGH THE SCHOTTKY BARRIER

The Schottky barrier[40,41] between a metal and a semiconductor is created by redistribution of charges in the space charge layer. We denote the barrier height measured from the Fermi level of the metals by ϕ_B, and its thickness as d. For uniformly n-doped semiconductor the barrier shape is approximately parabolic, and the depletion width d is the distance between the interface and the onset of the bulk flat-band region.

For Fe/GaAs junction[14] we will employ a value of ϕ_B=0.8 eV. For homogeneous doping $n_0<10^{17}$ cm^{-3} we have the depletion width $d>100$ nm. For such a wide barrier the tunneling current is negligible, and the current is due to purely classical thermionic emission[41] which depends on temperature and the barrier height, not on its width or shape. Even if this current is spin polarized, its total density is too small to create an appreciable spin accumulation. For higher n_0 the tunneling dominates the transport through the junction, but only for extremely high bulk doping levels ($n_0\sim10^{19}$ cm^{-3}) we have $d\approx10$ nm resulting in appreciable current densities. In order to achieve such thin barriers yet with the bulk of the semiconductor having the carrier density less than 10^{19} cm^{-3}, a strongly inhomogeneous doping profile has to be used near the interface.[13,14,15] Spin injection from Fe into GaAs with bulk $n_0\sim10^{16}$ cm^{-3} has been observed[9,11,17] only in such heavily doped junctions, in which the first 15 nm of semiconductor beneath the interface is doped with $n_d=5\cdot10^{18}$ cm^{-3} donors.

In general, the doping of the interface results in a creation of a potential well close to the barrier.[42,43,44] Even if there is no well in equilibrium, at high forward bias when less electrons need to be depleted from the semiconductor, the well creation is inevitable. In Sec. II B we show that the presence of bound states in this well can have a profound effect on spin extraction from the semiconductor.

A. Spin injection

Theoretical analysis of spin injection from metals into semiconductors has shown[45,46,47] that the junction with large resistance (a tunneling barrier) is necessary for the current to be polarized. More precisely, since the spin-depth conductance of the semiconductor $G_{\rm sc}=\sigma/L$ (with conductivity σ and spin diffusion length L) is much smaller than its metal counterpart $G_m=\sigma_m/L_m$, for spin injection to occur the junction conductance G has to fulfill $G\leq G_{\rm sc}$. In such a case the spin polarization of the current at the interface is determined by the spin-selectivity of the barrier, $\Delta G=G_+-G_-$, in which G_s are the conductances for spin $s=\pm$ (along the quantization axis given by magnetization of the ferromagnet). This "conductivity mismatch" effect was actually first analyzed in 1987 by Johnson and Silsbee.[48] From experiments on Fe/GaAs, $\Delta G/G\leq 0.3$ was deduced for spin injection.[11] We also stress that although the barrier with $G\ll G_{\rm sc}$ gives spin-polarized currents, the total current density can be too small to create an appreciable spin accumulation in the semiconductor.[47,49,50] A rule of a thumb is that $G\sim G_{\rm sc}$ leads to efficient spin injection (i.e. resulting in large spin accumulation), but, strictly speaking, the geometry of a system has to be taken into account when choosing the optimal barrier parameters.[49]

An important quantity in the description of spin transport is a spin-dependent electrochemical potential $\mu_s(\mathbf{x})$. It is defined as

$$\mu_s(\mathbf{x}) = \mu_s^c(\mathbf{x}) - e\phi(\mathbf{x}) \ , \qquad (1)$$

where μ_s^c is the chemical potential of electrons with spin $s=\pm$, ϕ is the electrostatic potential, and the elementary charge $e>0$. The spin splitting of the electrochemical potential, $\Delta\mu=\mu_+-\mu_-$, corresponds to the presence of non-equilibrium spin density (spin accumulation). In a non-magnetic material $\Delta\mu\neq 0$ means $\Delta n= n_+-n_-\neq 0$, where n_s is the density of electrons of spin component s.

In Fig. 1a we show the energy diagram of the Schottky barrier. We define the bias eV applied to the junction as the difference between the average electrochemical potential in the flat-band region $\mu=(\mu_+ + \mu_-)/2$ and metal's μ^m. $V>0$ (<0) is forward (reverse) bias corresponding to electrons going from (into) the semiconductor. This definition of V is convenient in the case of spin accumulation small enough for μ_s to be linearly proportional to the nonequilibrium parts of the spin densities δn_s, see Sec. III. Then, because of quasi-neutrality[51] we have $\delta n_+ + \delta n_- = 0$ and μ is equal to the equilibrium chemical potential in the semiconductor.

A schematic picture of spin injection and extraction through Schottky barriers is shown in Fig. 1b. The junctions are much more resistive than the semiconductor channel, so that the electrochemical potential shows discontinuities at the barriers. Because of this and the large difference of conductivities of the semiconductor and the ferromagnet, we can disregard both spatial and spin dependence of μ_s in the ferromagnet, and use a single value of chemical potential $\mu^{\rm m}$. The current injection occurs because of tunneling of electrons from the metal into the semiconductor, described[40] by spin-dependent transmission coefficient of the particle flux $T_s(k_x, \mathbf{k}_\parallel)$, with k_x the wave-vector in the direction of the interface, and $\mathbf{k}_\parallel$ the in-plane wave-vector, which we assume conserved (spec-

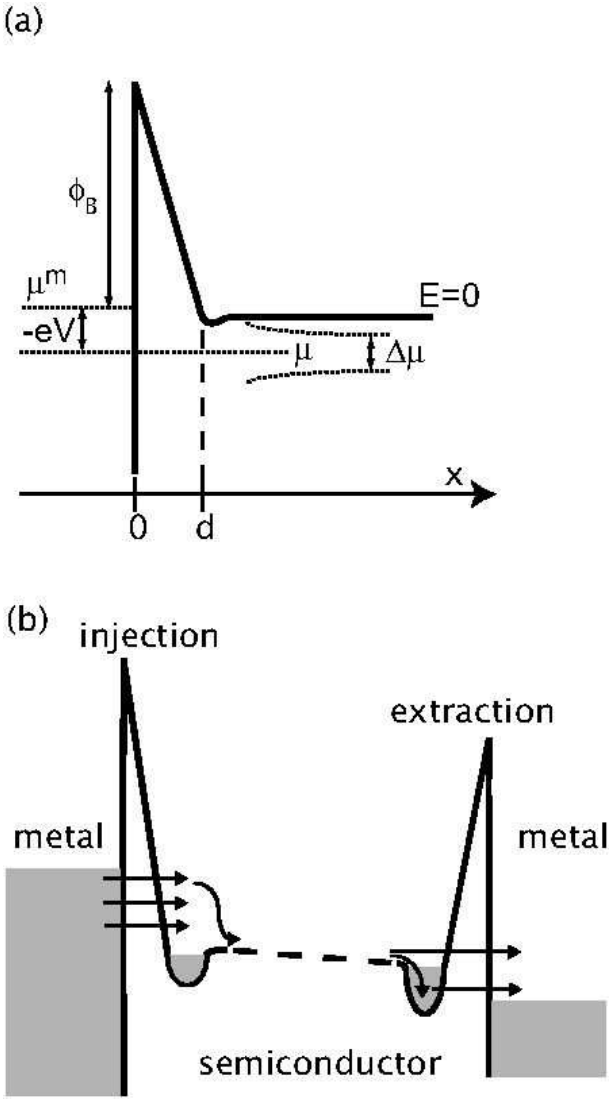

FIG. 1: (a) Heavily doped Schottky junction at reverse bias. The semiconductor is non-degenerate (at room temperature). μ is the average electrochemical potential at the onset of the flat-band region, and $\Delta\mu$ is the spin accumulation. (b) Schematic picture of current flow from the ferromagnetic injector down to the ferromagnetic spin-extracting drain. The potential wells filled with carriers near the interfaces are created by the inhomogeneous doping profile (heavy n^+ doping near the interface). For extraction, two routes are drawn: a direct tunneling from the bulk of the semiconductor (elastic process) and tunneling of the electrons from the potential well into the magnet sustained by capture of bulk electrons (inelastic process).

ular transmission).

We neglect the atomic structure of the Fe/GaAs interface,[15,22,52] and use a simplified band-structure for the bulk ferromagnet with a single spin-split band with spin-dependent Fermi velocities $v_{m,s}$. For iron, a model with effective mass m_m equal to the free-electron mass and Fermi wave-vectors k_+^m=1.1 Å^{-1} (k_-^m=0.42 Å^{-1}) for majority (minority) electrons has been widely used.[53,54] Due to the assumption of specular transmission only the electrons having $v_{m,s}^x \approx v_{m,s}$ can tunnel into the Γ valley of the semiconductor's conduction band. We define the imaginary wave vector within the barrier κ and the corresponding velocity $v_b=\hbar\kappa/m_{sc}$ (with semiconductor effective mass m_{sc}). For high barrier and $m_{sc} \ll m_m$ considered here we have $v_b \gg v_{m,s}, v_{sc}$, with the transmitted electron velocity in the semiconductor v_{sc}. Within this model we obtain for the flux transmission coefficient:

$$T_s \approx \frac{v_{m,s}v_{sc}}{v_{m,s}^2+v_b^2}e^{-2\kappa d} \approx \frac{v_{m,s}v_{sc}}{v_b^2}e^{-2\kappa d} \equiv v_{sc}A_s e^{-2\kappa d} \ . \tag{2}$$

If we approximate the barrier by a square step of thickness d, then $\kappa=\sqrt{2m_{sc}(\phi_B+\mu-eV)}/\hbar$. For a triangular barrier the expression for κ has to be modified,[55] but the spin-dependent A_s factor remains the same. Consequently, electrons with larger velocity in the metal tunnel more efficiently into the semiconductor. In iron this translates into preferential injection of majority spins, which is in agreement with experiments.[17] Within this model we also expect that if Fe is replaced by a zinc-blende MnAs, because of the different ratio between the majority and minority spin wave-vectors,[56] the spin-selectivity of the junction will have opposite sign to the Fe case.

For large reverse bias ($|eV| \gg k_BT$) the injected current does not depend on the occupation function in the semiconductor, since most of the electrons tunnel from the metal into the states at least k_BT above the chemical potential in the semiconductor (see Fig. 1b). Up to a certain critical reverse bias the barrier thickness does not change much, only the well becomes more shallow. Above this critical bias the electrons start to be depleted from the bulk of the semiconductor. The wide depletion region created then was shown to be detrimental to spin injection.[57] Another reason for avoiding too large reverse biases is that hot electron injection is accompanied by enhanced spin relaxation in GaAs.[58]

B. Spin extraction in the presence of bound states near the interface

An analogous calculation of tunneling from the 3D states in the bulk of the semiconductor into the metal (spin extraction) gives the same spin selectivity, so that the spins parallel to the minority spin in Fe should be accumulated, contrary to the observation.[17] The experiments can be explained by including the presence of electrons localized in in the well near the interface, and considering a two-step process, in which tunneling of the electrons from the bound states into the ferromagnet is followed by vacant states being filled by decay of extended state electrons (carrier capture).

The spin-selectivity of the junction for free and localized electrons is explained in the following way. For free electrons, current conservation is well defined on both sides of the interface region (elastic scattering). As explained before, in reverse or in low forward bias the 'effective velocity' in the barrier dominates and the current scales with the electron's velocity in the metal side. On the other hand, for localized electrons the conservation of total reflection and transmission is irrelevant. Electrons escape from the well into the vacant states in the ferromagnet and the transmitted current scales with the decay rate of the bounded wave function. In this case, the decay is fastest when the electron's velocity in the ferromagnet matches the 'effective velocity' in the well (being inversely proportional to the well's width). Later we show, that in the case of Fe/GaAs one gets an antipodal spin-behavior for free and localized carriers.[21]

We denote the bulk doping density by n_0. The ultra-heavily doped region at the junction has width d and doping n_d. There is also a transition region of width d_{tr} where the donor density interpolates between n_0 and n_d. The conditions for the existence of the potential well are the folllowing:[21]

$$d \approx \sqrt{\frac{2\epsilon_r\epsilon_0\phi_B}{e^2n_d}} \ , \tag{3}$$

$$n_d \gg n_0 \ , \tag{4}$$

$$d_{tr} \sim \lambda_B \ , \tag{5}$$

where ϵ_r is the relative permittivity of the semiconductor and λ_B is the electron's de Broglie wavelength (typically ∼10 nm in GaAs quantum wells). The first equation determines the Schottky barrier thickness d, the second guarantees an excess of electrons in the transition region, and the third one is for the two-dimensional character of the electronic states in the well.

In Fig. 2a we show the results of the self-consistent calculation of Schrödringer and Poisson equations for the conduction band profile near the junction at 0.2 V forward bias using n_0=3.6 · 10^{16} cm^{-3}, n_d=5 · 10^{18} cm^{-3}, d=d_{tr}=15 nm and ϵ_r=12.6. These parameters are chosen to approximate the junctions used in the experiments.[17,18,19] At this bias three bound states are present in the well.

The process of electron escape from the well into the continuum in the ferromagnet is calculated in the following way.[21] At time t=0 the wave functions for spin s=± are identical, taken as the ith bound state, and they are equal to zero on the metal side. The time-dependent Schrödringer equations is then solved numerically using the potential from Fig. 2a. Inside the metal (iron) we use the same simplified model as before. For the calculation we have used a one-dimensional box of 200 nm width encompassing both the well and the inside of the

metal, and we have used discrete transparent boundary conditions to prevent reflections from the edges.[59] Fig. 2b shows the wave functions of the third quasibound state penetrating into the metal at times t=40 and 400 fs. The electrons with minority spin in Fe have bigger penetration amplitude, and this behavior persists for longer times and for all the bound states. The escape rate is practically constant in time (resulting in exponential decay of the quasibound state) and is given by

$$\frac{1}{\tau_{i,s}^{esc}} = -\frac{1}{\int_{box} dx|\psi_{i,s}(x,t)|^2}\frac{d}{dt}\int_{semiconductor} dx|\psi_{i,s}(x,t)|^2 \ . \quad (6)$$

Fig. 2c shows the escape rate from the first quasi-bound state versus the wave-vector in the metal k_m. The escape rate has maximum when the 'effective velocity' in the well matches the velocity in the metal: $k_m/m_m \sim \pi/(m_{sc}d_{tr})$. The values of Fermi wave-vectors which we use for iron are on the right side of the curve, where the escape rate decreases with k_m. Such behavior for high metal wave-vectors agrees with the extended WKB model for the alpha-particle decay,[60] in which the coupling between a quasi-bound state and the continuum scales with the inverse wave-vector in the continuum.

The spin-dependent current density $J_{2D,s}$ due to leakage of localized electrons is proportional to the areal electron density in the ith state $\tilde{n}_{i,s}$ (with energy above the metal's Fermi level) divided by the escape time: $J_{2D,s} \propto \sum_i \tilde{n}_{i,s}/\tau_{i,s}^{esc}$. The spin relaxation time in the well is of the order of tens of ps,[61] whereas the escape time is ~1 ns, so that we have little spin accumulation in the well: $\tilde{n}_{i,s} \simeq \tilde{n}_i/2$. The electron which escapes from the well into the magnet is replenished by an electron with the same spin from the bulk region due to spin-conserving capture process of free electrons by the well, e.g. by emission of longitudinal optical phonons or carrier-carrier scattering with degenerate electrons in the well. These processes are much faster than the spin relaxation time in the well.[62] Thus, the bulk region is left with more spin-up (down) electrons if it provides the well with more spin-down (up) electrons. The necessity of the capture process is consistent with the longitudinal optical phonon signature in the low temperature conductance measurement of Fe/GaAs by Hanbicki et al.[11] The presence of this signature for the forward bias had been an open question, and our model suggests a possible explanation.

Apart from the current J_{2D} due to the escape from the well, there is always some current J_b due to direct tunneling between the bulk of the semiconductor and the metal. Fig. 2d shows the contributions to the total current due to the elastic and inelastic processes versus the bulk doping n_0, calculated at zero temperature. The transmission from the bulk states is calculated for the self-consistent potential using the transfer matrix method, including the resonant behavior of free electrons due to the well potential.[63] Since this potential is weakly affected by changing n_0 as long as $n_0 \ll n_d$, the J_{2D} current increases only by 10% in the shown range of n_0. On the other hand,

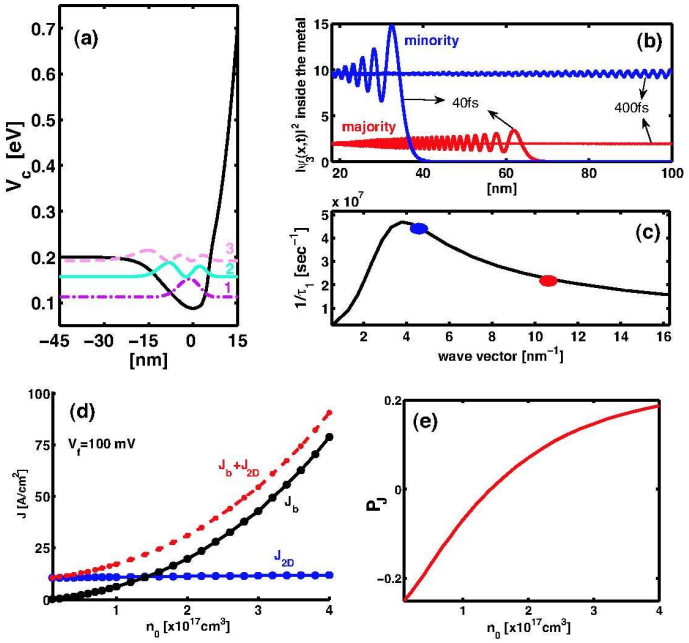

FIG. 2: (a) The self-consistent conduction band potential in the semiconductor for 0.2 V forward bias with the wave functions of the three bound states. (b) Spin-dependent amplitudes of the wave function penetrating into the ferromagnet after 40 and 400 fs. (c) Escape rate from the third bound state versus the wave-vector in the metal. The upper (lower) mark refers to the minority (majority) electrons in Fe. (d) Extracted current density as a function of the backround doping n_0 at zero temperature. J_b and J_{2D} denote current due to free and localized electrons, respectively, and $J_b + J_{2D}$ denotes the sum of the two terms (the total current). (e) Spin polarization of the total current. Panels (d) and (e) are adapted from Ref. 20.

J_b depends strongly on n_0: as the chemical potential in the bulk increases with n_0, the number of carriers which can tunnel into the metal increases. Fig. 2e shows the spin polarization of the total current $P_J = (J_+ - J_-)/J$. The critical background doping at which P_J=0 is $1.5 \cdot 10^{17}$ cm^{-3}. This is not exactly the density at which J_b=J_{2D} because $|P_{J_b}|$ and $|P_{J_{2D}}|$ are slightly different.

Because the effective spin selectivity of the junction depends on the carrier density and the bending of the conduction band, it can be controlled by voltage in the electrical spin switch.[21] In a semiconductor channel of thickness h~100 nm, a voltage applied to a back-gate deposited on the opposite side of the channel to the ferromagnetic contact can be used to manipulate the density of free electrons below the magnet. By varying this back-gate voltage V_G in a properly designed structure it is possible to switch between the transport regimes dominated by tunneling from the bulk and escape from the well, and thus change the sign of the spin accumulation in the semiconductor.[21]

C. Spin-dependent conductance at low bias

Now let us analyze the conductance of the interface with a very shallow well at small bias (an "optimally doped" barrier). We concentrate on the room-temperature case relevant for potential applications, and take the bulk of semiconductor as non-degenerate. An example of a doping profile yielding such an interface is the δ-doping,[42,43,44] in which a single monolayer of a semiconductor material near the interface is doped with a donor density impossible to achieve in the bulk material. When a δ-doping layer is placed at a distance d_0 from the interface, and its planar density is $n_{2D}{=}\epsilon_r\epsilon_0(\phi_B+\mu)/4\pi e^2 d_0$, then the barrier shape is triangular, there is no well at zero bias, and the barrier width is d_0. For $d_0{=}5$ nm, $\phi_B{=}0.8$ eV, and $\mu{=}{-}0.1$ eV (corresponding to bulk $n{=}10^{16}$ cm^{-3}), we get $n^0_{2D}{\approx}10^{13}$ cm^{-2}.

For the "optimally doped" contact only the elastic transport channel is present, and we can derive an expression[55] for the current with spin s. In the regime of bias $|eV|$, $|\mu^m-\mu_s|$, and $|\mu_s-\mu|$ smaller than k_BT the formulas for $j_s(V,\mu_s)$ can be linearized around $V{=}0$, and we obtain for the spin currents:

$$j_s \;\approx\; \frac{G_s}{e}(\mu_s^m-\mu_s)\;, \tag{7}$$

$$G_s \;=\; \frac{4e^2}{m_{\rm sc}}A_s e^{-2\kappa d}\;n_0\;, \tag{8}$$

where G_s is the barrier conductance at low bias, the spin-dependence of which comes from the A_s factor. As discussed above, the ratio G_+/G_- is equal to the ratio of the velocities of carriers with different spin in the ferromagnet, which is approximately 2 in our model in agreement with spin-LED experiments.[9,11] For $n_0{=}10^{16}$ cm^{-3} and $d_0{\approx}5$ nm we obtain G_s of the order of 10^3 Ω^{-1}cm^{-2}. In the following sections, we will use the above model of spin-dependent properties of the junction to model how the spin accumulation can be sensed electrically by a contact kept at low bias.

III. SPIN ACCUMULATION IN THE DIFFUSIVE SPIN VALVE

We work in the diffusive regime, in which the spin relaxation time τ_{sr} is much longer than the momentum scattering time. Then, from the Boltzmann equation we can derive the spin diffusion equation[64,65,66,67] for the non-equilibrium parts of the spin densities δn_s. In a paramagnetic and non-degenerate semiconductor the electrochemical potential μ_s defined in Eq. (1) is given by

$$\mu_s = k_BT\ln\Big(\frac{n_0/2+\delta n_s}{n_0/2}\Big){-}e\phi \;\simeq\; k_BT\frac{\delta n_s}{n_0/2}{-}e\phi\;, \tag{9}$$

where n_0 is the total carrier density, and the second expression is the linear approximation valid for $|\Delta\mu|{<}k_BT$ (equivalently $|\delta n_s|{<}n_0/2$). Here we concentrate on the linear regime and low electric fields,[68] so that we can write the diffusion equation for the spin-splitting of the electrochemical potentials:

$$\nabla^2\mu_s = \frac{\mu_s-\mu_{-s}}{2L^2}\;, \tag{10}$$

where the spin diffusion length is defined in terms of diffusion constant D and spin relaxation time by $L{=}\sqrt{D\tau_{sr}}$. For the spin-s current in the paramagnetic semiconductor we have

$$\mathbf{j}_s = \frac{\sigma_s}{e}\nabla\mu_s = \sigma_s\mathbf{E}+eD\nabla n_s\;, \tag{11}$$

where the conductivity for spin s is $\sigma_s{=}n_s e\nu$ with ν being the mobility, and $\sigma_+{\simeq}\sigma_-$ to the first approximation in the linear regime. The only way for the semiconductor to support a non-zero spin polarization of the current is by creating a net spin density ($n_+{\neq}n_-$ corresponding to $\Delta\mu{\neq}0$).

In the spin valve the current is passed through a paramagnetic channel between two ferromagnetic contacts. We assume collinear magnetizations, oriented either parallel (P) or antiparallel (AP) with respect to each other. If the distance between the contacts is smaller than spin diffusion length L, the spin accumulation in the channel depends on the alignment of the magnets. Provided that the spin transport mechanism is the same for injection and extraction, in P configuration the same spin species is preferentially injected and extracted. The spin accumulation has opposite signs in the neighborhood of the two contacts, and by $|\Delta\mu^P|$ we denote the magnitude of spin splitting near the junctions. In the AP configuration, spins of opposite directions are more easily injected and extracted, resulting in large and nearly uniform spin accumulation: $|\Delta\mu^{AP}|{\gg}|\Delta\mu^P|$. If the mechanisms of spin injection and extraction are different, and the spin selectivities of injecting and extracting junctions are opposite as described in Sec. II B, the labels P and AP refer not to the relative orientations of contact magnetizations, but to the spin accumulation patterns described above.

The magneto-resistive (MR) coefficient of the spin valve is commonly defined as $MR{\equiv}(I^P{-}I^{AP})/I^P$, where $I^{P(AP)}$ is the total current between the two terminals. A qualitative relation between the MR and the spin accumulation can be derived using the simple boundary conditions for currents from Eq. (8).

For the channel with relevant dimensions smaller than L, by balancing the net spin injection into the channel with the spin relaxation we obtain

$$MR = \frac{\Delta G}{G}\frac{\Delta\mu^{AP}}{eV} = \Big(\frac{\Delta G}{G}\Big)^2\Big(1+\frac{\mathcal{V}}{2\mathcal{A}L}\frac{G_{sc}}{G}\Big)^{-1}\;, \tag{12}$$

where $\mathcal{V}$ is the volume of the channel and $\mathcal{A}$ is the area of the contacts, which are assumed to both have the same G_s and $\mathcal{A}$ for simplicity. The MR depends on the ratio of $\Delta\mu^{AP}$ to the applied bias, which for small electric fields is just a geometry-dependent constant. For realistic parameters of a Fe/GaAs spin valve we obtain $MR{\ll}(\Delta G/G)^2$,

and a typical value of MR is about 1% after optimizing the system's geometry.[49] In a one-dimensional channel of length l we have $MR{\sim}(G/G_{sc})\cdot(L/l)$ which is quite small for realistic values of G and practical values of $l{\sim}100$ nm. On the other hand the ratio of spin splittings $|\Delta\mu^{AP}/\Delta\mu^{P}|{\sim}(2L/l)^2$ can be quite large even when MR is small. This large difference of spin accumulations in P and AP cases is not expressed in a two-terminal system in the most effective way by the magnetoresistive effect.

The MR of a one-dimensional spin valve has been calculated analytically[47] also using the boundary conditions from Eq. (8). The spin valve in the lateral geometry relevant for experiments[17,18,19] has been analyzed qualitatively[47,50] and quantitatively.[49] In the latter work an effective one-dimensional diffusion equation was derived, accurately describing the spin diffusion in a layer of material of thickness h smaller than the spin diffusion length L, and covered by contacts with junction conductances G smaller than the conductance σ/h of the underlying semiconductor layer. In a structure like the one shown in Fig. 3a, we calculate the spin diffusion by introducing the layer-averaged electrochemical potential $\xi_s(x)$ in the semiconductor channel: $\xi_s{=}\frac{1}{h}\int_0^h dy\,\mu_s(x,y)$. By integrating out the y dependence from Eq. (10) we obtain the approximate equation:

$$\frac{\partial^2\xi_s}{\partial x^2}=\frac{\xi_s-\xi_{-s}}{2L^2}+\frac{2G_s}{\sigma h}(\xi_s-\mu^m)\ , \qquad (13)$$

where the second term on the right-hand side is present only under the contacts, and μ^m is the electrochemical potential in the ferromagnet. This equation is derived using the boundary condition from Eq. (8), and assuming small electric fields and small spin accumulations (so that $\sigma_s{\approx}\sigma/2$). For Fe/GaAs structures with $G_s{\sim}10^3$ $\Omega^{-1}\mathrm{cm}^{-2}$ this approximate formalism gives results indistinguishable from exact numerical calculations, and all the results presented below are obtained using this approach.

IV. ELECTRICAL EXPRESSION OF SPIN ACCUMULATION IN MULTI-TERMINAL SYSTEMS

In the previous section we have seen that in the spin valve the patterns of spin accumulation in the semiconductor are qualitatively different for P and AP configurations, but the MR ratio does not directly reflect this feature. In order to achieve a more efficient electrical expression of spin accumulation one has to move beyond a passive two-terminal device such as spin valve, and consider a spin-transistor system in which additional external stimuli can control the magnetoresistive effects. Below we review several proposals of devices consisting of more than two ferromagnetic terminals connected to a semiconductor channel. Their common feature is the use of a ferromagnetic contact kept close to zero bias (Sec. II C), which is used to sense the spin accumulation in the semiconductor beneath it.

A. Magnetic Contact Transistor

The Magnetic Contact Transistor (MCT) consists of three ferromagnetic contacts deposited on top of the paramagnetic channel (see Fig. 3a). We concentrate on situation in which most of the current driven by the voltage V_L passes between the left (L) and middle (M) contacts, but other arrangements are possible.[69] The voltage V_R is adjusted to keep the R junction at low bias,[38] and we describe its spin-dependent conductance using Eq. (8). Alternatively,[70] the R terminal can be connected to a capacitor C, which adjusts the voltage of the R terminal so that there is no net charge current in the steady state. We will refer to P (AP) configurations of the L and M magnets as corresponding to the spin accumulation patterns described before. In this section we keep the M magnet fixed, and consider the P and AP alignments of the L magnet with respect to M.

Let us first consider a situation in which the R terminal is inactive. Then the L and M contacts constitute a spin valve with voltage V_L applied to it. For P and AP alignments of L and M the I_L current is practically the same, but the spin splitting of layer-averaged electrochemical potential in the channel $\Delta\xi$ varies between two very different values. Beneath the injecting and extracting contacts we have $|\Delta\xi^{AP}/\Delta\xi^{P}|{\propto}(2L/l)^2$, with the effective length of the active channel covered by L and M terminals $l{\approx}w_d{+}w_L{+}w_M$. The spins accumulated beneath the M terminal diffuse out to the right, but if $w_d{\ll}L$ the spin accumulation beneath the R magnet is practically the same as beneath the M contact.

The operational principle of the "static" MCT relies on the fact that we actively control the V_R voltage.[38] In either P or AP alignment we bias the R terminal so that $I_R{=}0$. If we then flip the L magnetization, *a finite I_R current will flow.* This is a consequence of large spin accumulation in AP configuration, and spin selectivity of the R junction ($\Delta G_R{\neq}0$). Using $|\Delta\xi^{P}|{\ll}\left|\Delta\xi^{AP}\right|$ the "on" current is given by

$$|I_R^{on}|\approx\left|\frac{\Delta G_R}{e}\frac{\Delta\xi^{AP}}{2}\right|\mathcal{A}\ . \qquad (14)$$

Thus, we have found a way to *digitize the MR effect in the R contact.* Instead of some finite ratio of P and AP currents, we can have zero current for one and a finite current for the other configuration. Even after taking the voltage noise in the system into account, the "on" and "off' currents should be easily discernible for realistic parameters of Fe/GaAs system.[38] This digitization of the magnetoresistance had been observed recently in MnAs/GaAs three-terminal structure.[69]

The digitization holds for the MR effect measured in the third (R) terminal. The larger currents in the other

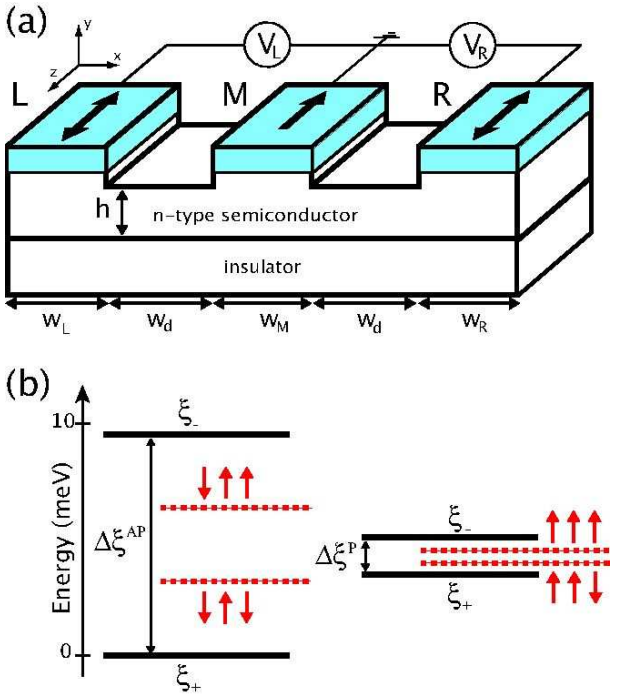

FIG. 3: (a) The three-terminal Magnetic Contact Transistor (MCT). The outer edges if the channel are removed in order to confine the spin accumulation under and between the contacts.[49] The R contact is connected either to a controllable voltage V_R, or to a capacitor C which maintains zero steady state current in this terminal. (b) A schematic picture illustrating the principle of the MCT operation. The solid lines are the electrochemical potentials (ξ_s) in the channel beneath the R contact for AP and P alignments of the L and M terminals. The dashed lines show the values of the electrochemical potential inside the R contact for which the I_R current is quenched for a given alignment of all magnetizations (represented by three arrows). The energy scale and $\Delta\xi^{AP}/\Delta\xi^{P}$ ratio correspond to an MCT with barrier conductances G=10^4 Ω^{-1}cm^{-3}, dimensions w_L=w_M=w_R=400 nm, w_d=200 nm, h=100 nm, and V_L=0.1 V.

two (L and M) have a small relative change when we alternate between P and AP configurations. Yet these contacts do almost all of the job of injecting and extracting spin-polarized currents. We can say that we have transferred the magneto-resistive effect to the third contact, where we can tune it by V_R voltage. We have called this *spin transference*.[38] An alternative term of "transferable magnetoresistance" underlines the connection to standard transistors.

To sketch the derivation of the above effect we write the spin dependent electrochemical potentials underneath the R terminal as

$$\xi_\pm = \xi \pm \frac{1}{2}\Delta\xi \ , \tag{15}$$

where ξ is the average value of electrochemical potential. If we apply any voltage V_R, the situation inside the channel will change in general. However, we are interested in V_R such that there is only a small (possibly zero) I_R current. Then the spin accumulation determined by the larger I_L injected into the channel remains practically unaffected. For such a voltage applied to R we have the current density entering the R contact:

$$j_R = \frac{G_R}{e}(\mu_R - \xi) - \frac{\Delta G_R}{e}\frac{\Delta\xi}{2} \ , \tag{16}$$

where μ_R=$-eV_R$, G_R is the total conductance of the R junction, and ΔG_R=$G_+^R - G_-^R$ is its spin selectivity. The corresponding spin current density Δj=$j_+ - j_-$ is

$$\Delta j_R = \frac{\Delta G_R}{e}(\mu_R - \xi) - \frac{G_R}{e}\frac{\Delta\xi}{2} \ . \tag{17}$$

We denote by μ_0 the electrochemical potential in R magnet that quenches the total current in this contact:

$$\mu_0 = \xi + \frac{\Delta G_R}{G_R}\frac{\Delta\xi}{2} \ . \tag{18}$$

Plugging this μ_0 for one L/M alignment into Eq. (16) with $\Delta\xi$ corresponding to the other L/M alignment we obtain Eq. (14). Depending on the alignment of the L and R magnets, the V_R voltage which corresponds to I_R=0 takes on four possible values denoted by dashed lines in Fig. 3b. When the R terminal is connected to the capacitor, we have four possible charge states of the capacitor in the steady state. We discuss the transient currents driven by L or R magnetization dynamics for this case in Sec. IV B below.

In the "off" state, when V_R is adjusted so that the net I_R=0, there is a non-zero spin current flowing into the R terminal:

$$\Delta j_R^{off} = \frac{\Delta\xi^{P,AP}}{2e}\frac{\Delta G_R^2 - G_R^2}{G_R} \ . \tag{19}$$

The electrons with opposite spins flow in the opposite directions, giving zero charge current, but adding to a net flow of spin polarization. A similar effect was predicted in a lateral structure with non-magnetic source and drain and two ferromagnetic gates, into which the current could leak.[33] A finite spin current entering a ferromagnet can lead to reversal or precession of the magnetization due to spin-transfer torque if the polarization of injected spins is non-collinear with the magnetization axis of the magnet.[71] This effect has been observed in an all-metallic system,[72] in which the magnetization of a floating terminal (zero net charge current through it) was switched by a pure spin current. However, in our case the relatively low carrier density in the semiconductor together with the resistive contacts cannot transfer enough angular momentum for such switching to occur.

A system similar to the MCT has been known for some time in the field of all-metal magnetoelectronics as a non-local spin valve.[73,74,75] However, the third contact in the non-local spin valve is used as a passive floating terminal (essentially a spin dependent voltage probe). In the MCT all the contacts are active terminals controlled by

applied voltages. The possibility of control is closely related to the use of the non-degenerate semiconductor as a paramagnetic channel. Due to very small concentration of carriers compared to metals, spin injection can lead to spin splittings of electrochemical potentials of the order of milivolts in the channel. Then, voltages supplied with mV accuracy can efficiently tune the magnetoresitive effect measured in one of the terminals.

B. Electric readout of magnetization dynamics

The MCT can also be used for electric measurement of magnetization dynamics and dynamical readout of magnetization alignment. With the R contact connected to a capacitor C there is zero I_R current in the steady state.[70] For any alignment of all the magnetizations, the charge on the capacitor adjusts itself so that the electrochemical potential in the R contact is equal to the current-quenching μ_0, and there is no need for external voltage tuning. When either the L or the R magnet starts to reverse due to an application of an external magnetic field pulse, the potential in the R contact changes between two steady-state values (dashed lines in Fig. 3) corresponding to the initial and final alignments of the magnetizations. The measurement of the accompanying transient $I_R(t)$ current recharging the capacitor allows for electrical monitoring of magnetization dynamics. Alternative application is a dynamical readout of the L/M alignment. In the P case, the 2π rotation of the R magnet results in the $I_R(t)$ current oscillation of much smaller amplitude than for the AP case (see Fig. 4).

The on-chip manipulation of L and R magnetizations is possible using the architecture[76,77] of Magnetic Random Access Memory (MRAM). In MRAM the nanomagnets (with typical size similar to what we use in our modeling) arranged in a square array are addressed using a network of current-carrying wires positioned above and below the magnets. Pulses of current generate time-dependent magnetic fields through Ampere's law, and these field can be used to switch each of the magnets separately.

The capacitor RC time (with R being of the order of the junction resistance, as they are the most resistive elements in the circuit) has to be at most comparable to the magnetization dynamics time-scale. For $G\sim10^4\ \Omega^{-1}\mathrm{cm}^{-2}$ and junction area of one $\mu\mathrm{m}^2$, the capacitance C=40 fF used below results in RC time of about a nanosecond. In all-metallic systems, in which the junctions are much less resistive, the RC time is not a problem. However, typical spin accumulation in paramagnetic metal corresponds to $\Delta\mu$ (and consequently the voltage swing on the capacitor) of less than μV.[74,75] Then, for the transient current to be measurable one has to use a nearly macroscopic capacitor, which rules out an application in integrated circuits. Again, the small carrier density in a semiconductor (allowing for $\Delta\mu\sim10$ mV) is indispensable.

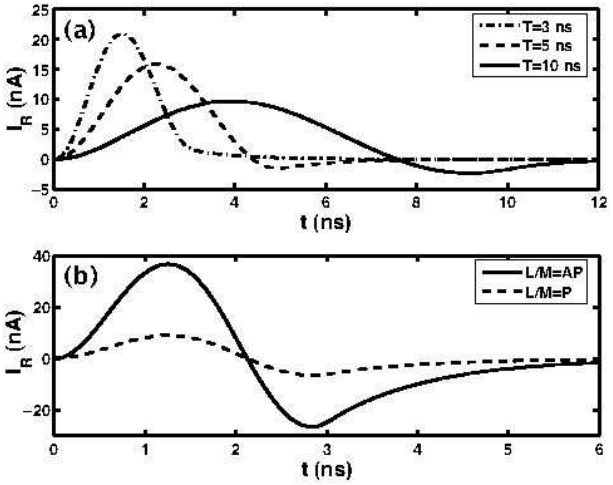

FIG. 4: (a) R current signal for reversal of L magnetization occurring on time-scale of 3, 5 and 10 ns starting from AP alignment of L relative to M magnet. (b) R current signal for 2π rotation of R magnet for P and AP alignments of L and M magnets. The period of rotation is 3 ns. The conductance of the barriers G=$10^4\ \Omega^1\mathrm{cm}^{-2}$. The area of a junction is 1 $\mu\mathrm{m}^2$, and the barrier thickness is taken to be 10 nm, resulting in junction resisitance R_B=10 kΩ and capacitance C_B=10 fF. The external capacitance is C=40 fF. The channel is GaAs at room temperature, with carrier density n_0=$10^{16}\mathrm{cm}^{-3}$. Adapted from Ref. 69.

In order to model the transient behavior we add the time dependence to the formalism of lateral spin diffusion. We are interested in time-scales of a least tens of picoseconds. The fastest magnetization reversal time is about 100 ps,[78] and magnetization switching times used in commercial devices are of the order of a nanosecond. Thus, we use an adiabatic approximation with respect to the processes occurring on a much shorter (subpicosecond) time scales: the momentum scattering and dielectric relaxation.[51]

The time-dependent diffusion equation for spin splitting of the layer-averaged electrochemical potential $\Delta\xi$ is

$$\frac{\partial\Delta\xi}{\partial t}=D\frac{\partial^2\Delta\xi}{\partial x^2}+\frac{\beta_i(t)}{\tau_{sr}}(\mu_i^m-\xi)-\frac{\alpha_i}{2\tau_{sr}}\Delta\xi-\frac{\Delta\xi}{\tau_{sr}}\ . \quad (20)$$

The $\alpha(\beta)$ dimensionless parameter is given by $2L^2(G_+{+}(-)G_-)/\sigma h$. The dynamics of magnetization is parametrized by $\beta(t)\sim\Delta G(t)$, which characterizes the contact polarization only along the z axis. If we deal with a coherent precession of magnetization then this is an approximation. In principle, one should treat the diffusion of spin accumulation treated as a vector quantity,[79] and take into account the noncollinearity of spins and the magnets in the tunneling process.[54,80,81] However, for tunneling barriers the non-trivial effects of this noncollinearity are expected to be small,[80,81] and the only thing that matters is the average polarization along the z direction. Then we can model the influence

of the contact with magnetization making an angle θ with the z axis by assuming that $\beta \sim \Delta G \cos\theta$. On the other hand, if the magnetization reversal is incoherent (e.g. proceeding by nucleation of domains with opposite magnetization), the parameter $\beta(t)$ describes an area average of spin-selectivity of magnetically inhomogeneous contact, and it is proportional to the z component of the contact's magnetization.

The dielectric relaxation (about 100 fs for non-degenerate semiconductor with $n_0 = 10^{16}$ cm^{-3}) is much faster than the time-scale of magnetization dynamics and spin diffusion, so we assume quasi-neutrality in the channel at all times ($\delta n_+(t) + \delta n_-(t) = 0$). In the linear regime under consideration (when $\Delta\xi < k_B T$) the average electrochemical potential $\xi = (\xi_+ + \xi_-)/2$ is equal to $-e\phi$. At every moment of time ξ fulfills the Laplace equation with boundary conditions given by currents at the interfaces. In the time-dependent case these include also displacement currents connected with charging of the barrier capacitance C_B. A Schottky barrier is a dipole layer, and its capacitance can have a strong effect on dynamics of currents on time scales of interest here. With the displacement current taken into account, the boundary condition for spin current is:

$$j_s = \frac{G_s}{e}(\mu^m(t) - \xi_s(t)) + \frac{c_B}{2e}\frac{\partial}{\partial t}(\mu^m(t) - \xi(t)) \ , \quad (21)$$

where c_B is the barrier capacitance per unit area. The second term in the above equation represents the carriers which flow towards the barrier, but do not tunnel through it. Instead, they stay in the semiconductor close to the barrier, making the depletion region slightly thinner or wider. The charge involved in this process is negligible compared to the charge already swept out from the semiconductor, so we can keep c_B constant. For small spin splitting (so that the conductivities $\sigma_+ \simeq \sigma_-$) the same amount of carriers of each spin is going to be brought from the channel into the barrier, and the displacement current is the same for each spin in Eq. (21). For layer-averaged ξ we get then

$$\frac{\partial^2 \xi}{\partial x^2} = -\frac{\alpha_i}{2L^2}(\mu_i^m - \xi) + \frac{\beta_i(t)}{4L^2}\Delta\xi - \frac{c_B}{\sigma h}\frac{\partial}{\partial t}(\mu_i^m - \xi) \ , \quad (22)$$

with the right hand side of Eq. (22) non-zero only under the contacts. The magnetization dynamics of i^{th} contact translates into time-dependence of β_i, driving the spin diffusion in Eq. (20) and electric potential in the channel in Eq. (22). From ξ_s we calculate the current $I_R(t)$ charging the capacitor C. The electrochemical potential of the R terminal $\mu_R = -eV_R$ changes according to $dV_R/dt = I_R/C$. Examples of calculations for two possible modes of operation (sensing the L dynamics and reading out the L/M alignment) are shown in Fig. 4.

C. Reprogrammable Magneto-Logic Gate

The same physical principle of operation can be harnessed to achieve a higher level functionality. In Fig. 5a we present a scheme of a five-terminal system,[39] in which the electric sensing of spin accumulation is used to perform a logic operation, i.e., two bits of input are converted into a binary output signal. This is a reprogrammable magneto-logic gate (MLG). Spintronics logic gates have been proposed in purely metallic systems,[82,83,84,85,86,87] but ours is the first proposal which employs semiconductors as active elements of the system.

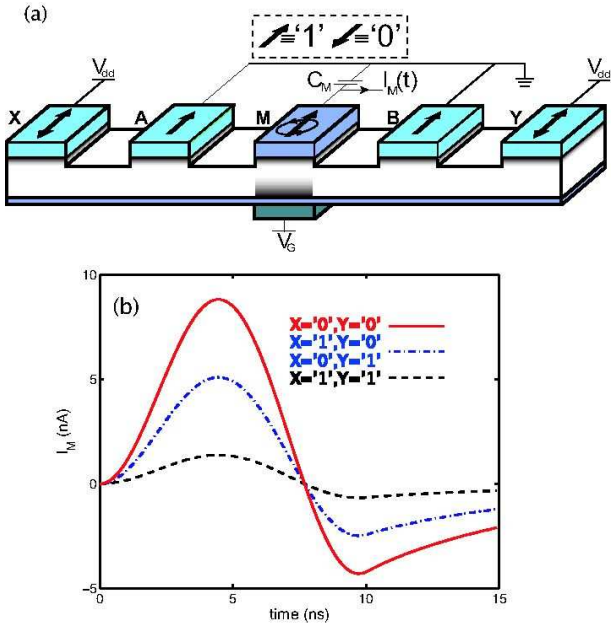

FIG. 5: (a) A five-terminal magneto-logic gate (MLG). The logic inputs '0' and '1' are encoded by magnetization direction of the A,B,X,Y terminals (see text for details). As shown here, the gate is set to work as a NAND operation between X and Y (A and B are fixed to '1' values). In the read-out phase the magnetization of the middle (M) terminal is rotated by 2π, or the back-gate voltage V_G is increased. (b) The $I_M(t)$ transient current triggered by the rotation of the M magnetization. The small signal for X='1', Y='1' corresponds to logical '0' output. Adapted from Ref. 38.

The system presented in Fig. 5a works in the following way. The charge currents are flowing between two pairs of terminals (X and A, Y and B), between which the bias V_{dd} is applied. Depending on the alignment of these pairs of magnets, different patterns of spin accumulation are created in the channel: if both X/A and Y/B are AP the spin accumulation underneath M is large; if only one pair of contacts is AP the spin accumulation is approximately two times smaller, and if both pairs are P there is a very small $\Delta\xi$ beneath the M terminal. The M contact is used to directly express the differences in the average spin accumulation beneath it.

The logical inputs are encoded by magnetization directions of A, B, X, and Y terminals. We will concentrate on the case in which A and B magnetizations are preset, defining the logic function of the gate. This reprogrammability is an important feature of magnetization-

based logic. X and Y are then the logic inputs, and the output is generated when the M magnet is rotated by 2π, triggering a transient $I_M(t)$ current of amplitude proportional to the spin accumulation in the middle of the channel. Let us focus on the example of the NAND gate, as any other logic function can be realized by using a finite number of such gates. For the NAND operation, A and B magnets are set parallel to each other in the direction defining the logical '1'. The amplitude of the $I_M(t)$ oscillation is two times larger for X='0' and Y='0' compared to the case when one of them is '0' and the other is '1', and for '11' case the current is negligible. This is shown in Fig. 5b. The transient current can be captured by an external electronic circuit, and then used to control a suitable write operation applied to the magnetic contact of another gate.[39]

Instead of using magnetic field pulses to drive the 2π rotation of the M magnet, one can employ the idea of the spin switch outlined in Sec. II B, in which the M magnetization is pinned, and the profile of the conduction band beneath M is changed by applying a voltage pulse $V_G(t)$ to the back gate shown in Fig. 5a. V_G is chosen to deplete the electrons from the lower part of the channel, biasing them vertically towards the Schottky barrier. Thus, the effective spin selectivity of the M junction is switched as discussed in Sec. II B. This is qualitatively the same as reversing the M magnetization, and the transient current I_M should be generated. However, its quantitative calculation is much more involved than in the case of magnetization rotation, and it will be addressed in future work.

V. SUMMARY

We have reviewed the physics of spin injection and extraction through inhomogeneously doped Schottky barriers. We have paid special attention to the states localized close to the junction as a consequence of heavy doping near the interface, and we have shown that they play a crucial role in the recent spin extraction experiments. A junction held at low bias in the presence of spin accumulation in the semiconductor has been also analyzed, and how its spin-dependent properties could be used to electrically sense the spin accumulation in a semiconductor has been described. The multi-terminal systems (a three-terminal transistor and a five-terminal logic gate) which we have described rely only on spin-selectivity of the junctions and the presence of the spin accumulation. As such, they are ideal candidates for spintronics devices working at room temperature and, possibly, in silicon.

Acknowledgments

This work was supported by the NSF under Grant No. DMR-0325599. We are grateful to P. Crowell, M. Johnson, and B. Jonker for helpful discussions.

* Electronic address: cywinski@physics.ucsd.edu

[1] M. Johnson and R. H. Silsbee, Phys. Rev. Lett. **55**, 1790 (1985).
[2] M. Johnson and R. H. Silsbee, Phys. Rev. B **37**, 5326 (1988).
[3] I. Žutić, J. Fabian, and S. D. Sarma, Rev. Mod. Phys. **76**, 323 (2004).
[4] R. Fiederling, M. Keim, G. Reuscher, W. Ossau, G. Schmidt, A. Waag, and L. W. Molenkamp, Nature **402**, 787 (1999).
[5] Y. Ohno, D. K. Yound, B. Beschoten, F. Matsukura, H. Ohno, and D. D. Awschalom, Nature **402**, 790 (1999).
[6] M. Oestreich, J. Hübner, D. Hägele, P. J. Klar, W. Heimbrodt, W. W. Rühle, D. E. Ashenford, and B. Lunn, Appl. Phys. Lett. **74**, 1251 (1999).
[7] B. T. Jonker, Y. D. Park, B. R. Bennett, H. D. Cheong, G. Kioseoglou, and A. Petrou, Phys. Rev. B **62**, 8180 (2000).
[8] H. J. Zhu, M. Ramsteiner, H. Kostial, M. Wassermeier, H.-P. Schonherr, and K. H. Ploog, Phys. Rev. Lett. **87**, 016601 (2001).
[9] A. T. Hanbicki, B. T. Jonker, G. Itskos, G. Kioseoglou, and A. Petrou, Appl. Phys. Lett. **80**, 1240 (2002).
[10] J. Strand, B. D. Schultz, A. F. Isakovic, C. J. Palmstrom, and P. A. Crowell, Phys. Rev. Lett. **91**, 036602 (2003).
[11] A. T. Hanbicki, O. M. J. van't Erve, R. Magno, G. Kioseoglou, C. H. Li, B. T. Jonker, G. Itskos, R. Mallory, M. Yasar, and A. Petrou, Appl. Phys. Lett. **82**, 4092 (2003).
[12] C. Adelmann, X. Lou, J. Strand, C. J. Palmstrom, and P. A. Crowell, Phys. Rev. B **71**, 121301 (2005).
[13] B. T. Jonker, Proceedings of the IEEE **91**, 727 (2003).
[14] C. Adelmann, J. Q. Xie, C. J. Palmstrom, J. Strand, X. Lou, J. Wang, and P. A. Crowell, J. Vac. Sci. Technol. B **23**, 1747 (2005).
[15] T. J. Zega, A. T. Hanbicki, S. C. Erwin, I. Žutić, G. Kioseoglou, C. H. Li, B. T. Jonker, and R. M. Stroud, Phys. Rev. Lett. **96**, 196101 (2006).
[16] J. Stephens, J. Berezovsky, J. P. McGuire, L. J. Sham, A. C. Gossard, and D. D. Awschalom, Phys. Rev. Lett. **93**, 097602 (2004).
[17] S. A. Crooker, M. Furis, X. Lou, C. Adelmann, D. L. Smith, C. J. Palmstrom, and P. A. Crowell, Science **309**, 2191 (2005).
[18] X. Lou, C. Adelmann, M. Furis, S. A. Crooker, C. J. Palmstrom, and P. A. Crowell, Phys. Rev. Lett. **96**, 176603 (2006).
[19] X. Lou, C. Adelmann, S. A. Crooker, E. S. Garlid, J. Zhang, K. M. Reddy, S. D. Flexner, C. J. Palmstrom, and P. A. Crowell, Nature Physics **3**, 197 (2007).
[20] Y. Imry, *Introduction to Mesoscopic Physics* (Oxford University Press, Oxford, 1997).
[21] H. Dery and L. J. Sham, Phys. Rev. Lett. **98**, 046602 (2007).

[22] A. N. Chantis, K. D. Belashchenko, D. L. Smith, E. Y. Tsymbal, M. van Schilfgaarde, and R. C. Albers, cond-mat/0707.3644 (2007).
[23] S. Datta and B. Das, Appl. Phys. Lett **56**, 665 (1990).
[24] Y. A. Bychkov and E. I. Rashba, J. Phys. C **17**, 6039 (1984).
[25] R. Winkler, *Spin-Orbit Coupling Effects in Two-Dimensional Electron and Hole Systems* (Springer-Verlag, Berlin, 2003).
[26] J. Schliemann, J. C. Egues, and D. Loss, Phys. Rev. Lett. **90**, 146801 (2003).
[27] M. E. Flatté and G. Vignale, Appl. Phys. Lett. **78**, 1273 (2001).
[28] J. Fabian, I. Žutić, and S. D. Sarma, Appl. Phys. Lett. **84**, 85 (2004).
[29] J. Fabian and I. Žutić, Phys. Rev. B **69**, 115314 (2004).
[30] I. Žutić, J. Fabian, and S. C. Erwin, J. Phys.: Condens. Matter **19**, 165219 (2007).
[31] K. C. Hall, W. H. Lau, K. Gündogdu, M. E. Flatté, and T. F. Boggess, Appl. Phys. Lett. **83**, 2937 (2003).
[32] C. Ciuti, J. P. McGuire, and L. J. Sham, Appl. Phys. Lett. **81**, 4781 (2002).
[33] J. P. McGuire, C. Ciuti, and L. J. Sham, Phys. Rev. B **69**, 115339 (2004).
[34] J. M. Anderberg, G. T. Einevoll, D. C. Vier, S. Schultz, and L. J. Sham, Phys. Rev. B. **55**, 13745 (1997).
[35] B.-C. Min, K. Motohashi, C. Lodder, and R. Jansen, Nature Materials **5**, 817 (2006).
[36] I. Appelbaum, B. Huang, and D. J. Monsma, Nature **447**, 295 (2007).
[37] B. T. Jonker, G. Kioseoglou, A. T. Hanbicki, C. H. Li, and P. E. Thompson, Nature Physics **3**, 542 (2007).
[38] H. Dery, Ł. Cywiński, and L. J. Sham, Phys.Rev. B **73**, 161307 (2006).
[39] H. Dery, P. Dalal, Ł. Cywiński, and L. J. Sham, Nature **447**, 573 (2007).
[40] E. Burstein and S. Lundqvist, eds., *Tunneling Phenomena in Solids* (Plenum Press, New York, 1969).
[41] S. M. Sze, *Physics of Semiconductor Devices* (John Wiley, New York, 1981).
[42] M. Zachau, F. Koch, K. Ploog, P. Roentgen, and H. Beneking, Solid State Commun. **59**, 591 (1986).
[43] J. M. Geraldo, W. N. Rodrigues, G. Medeiros-Ribeiro, and A. G. de Oliveira, J. Appl. Phys. **73**, 820 (1993).
[44] V. I. Shashkin, A. V. Murel, V. M. Daniltsev, and O. K. Khrykin, Semiconductors **36**, 505 (2002).
[45] G. Schmidt, D. Ferrand, L. W. Molenkamp, A. T. Filip, and B. J. van Wees, Phys. Rev. B **62**, R4790 (2000).
[46] E. I. Rashba, Phys. Rev. B **62**, R16267 (2000).
[47] A. Fert and H. Jaffrès, Phys. Rev. B **64**, 184420 (2001).
[48] M. Johnson and R. H. Silsbee, Phys. Rev. B **35**, 4959 (1987).
[49] H. Dery, Ł. Cywiński, and L. J. Sham, Phys. Rev. B **73**, 041306 (2006).
[50] A. Fert, J.-M. George, H. Jaffrès, and R. Mattana, IEEE Trans. Electron Dev. **54**, 921 (2007).
[51] R. A. Smith, *Semiconductors* (Cambridge University Press, Cambridge, England, 1978).
[52] M. Zwierzycki, K. Xia, P. J. Kelly, G. E. W. Bauer, and I. Turek, Phys. Rev. B **67**, 092401 (2003).
[53] J. C. Slonczewski, Phys. Rev. B **39**, 6995 (1989).
[54] C. Ciuti, J. P. McGuire, and L. J. Sham, Phys. Rev. Lett. **89**, 156601 (2002).
[55] V. V. Osipov and A. M. Bratkovsky, Phys. Rev. B **70**, 205312 (2004).
[56] Y. J. Zhao, W. T. Geng, A. J. Freeman, and B. Delley, Phys. Rev. B. **65**, 113202 (2002).
[57] J. D. Albrecht and D. L. Smith, Phys. Rev. B **68**, 035340 (2003).
[58] S. Saikin, M. Shen, and M.-C. Cheng, J. Phys.: Condens. Matter **18**, 1535 (2006).
[59] A. Arnold, M. Erhardt, and I. Sofronov, Commun. Math. Sci. **1**, 501 (2003).
[60] E. C. Kemble, *The Fundamental Principles of Quantum Mechanics* (Dover, New York, 1958).
[61] A. Malinowski, R. S. Britton, T. Grevatt, R. T. Harley, D. A. Ritchie, and M. Y. Simmons, Phys. Rev. B. **62**, 13034 (2000).
[62] B. Deveaud, J. Shah, T. C. Damen, and W. T. Tsang, Appl. Phys. Lett. **52**, 1886 (1988).
[63] M. D. Stiles, Phys. Rev. B. **48**, 7238 (1993).
[64] T. Valet and A. Fert, Phys. Rev. B **48**, 7099 (1993).
[65] S. Hershfield and H. L. Zhao, Phys. Rev. B **56**, 3296 (1997).
[66] L. Villegas-Lelovsky, J. Appl. Phys. **101**, 053707 (2007).
[67] Ł. Cywiński, Ph.D. thesis, University of California, San Diego (2007).
[68] Z. G. Yu and M. E. Flatté, Phys. Rev. B **66**, 235302 (2002).
[69] D. Saha, M. Holub, and P. Bhattacharya, Appl. Phys. Lett. **91**, 072513 (2007).
[70] Ł. Cywiński, H. Dery, and L. J. Sham, Appl. Phys. Lett. **89**, 042105 (2006).
[71] M. D. Stiles and J. Miltat, Top. Appl. Phys. **202**, 225 (2006).
[72] T. Kimura, Y. Otani, and J. Hamrle, Phys. Rev. Lett. **96**, 037201 (2006).
[73] M. Johnson, Science **260**, 320 (1993).
[74] F. J. Jedema, A. T. Filip, and B. J. van Wees, Nature **410**, 345 (2001).
[75] Y. Ji, A. Hoffman, J. E. Pearson, and S. D. Bader, Appl. Phys. Lett. **88**, 052509 (2006).
[76] G. A. Prinz, Science **282**, 1660 (1998).
[77] S. Tehrani, J. M. Slaughter, M. Deherrera, B. N. Engel, N. D. Rizzo, J. Salter, M. Durlam, R. W. Dave, J. Janesky, B. Butcher, K. Smith, G. Grynkewich, Proceedings of the IEEE **91**, 703 (2003).
[78] T. Gerrits, H. A. M. van den Berg, J. Hohlfeld, L. Bar, and T. Rasing, Nature **418**, 509 (2002).
[79] S. Saikin, J. Phys.: Condens. Matter **16**, 5071 (2004).
[80] A. Brataas, Y. V. Nazarov, and G. E. W. Bauer, Phys. Rev. Lett. **84**, 2481 (2000).
[81] A. Brataas, Y. V. Nazarov, and G. E. W. Bauer, Eur. Phys. J. B **22**, 99 (2001).
[82] R. P. Cowburn and M. E. Welland, Science **287**, 1466 (2000).
[83] A. T. Hanbicki, R. Magno, S.-F. Cheng, Y. D. Park, A. S. Bracker, and B. T. Jonker, Appl. Phys. Lett. **79**, 1190 (2001).
[84] A. Ney, C. Pampuch, R. Koch, and K. H. Ploog, Nature **425**, 485 (2003).
[85] D. A. Allwood, G. Xiong, C. C. Faulkner, D. Atkinson, D. Petit, and R. P. Cowburn, Science **309**, 1688 (2005).
[86] A. Imre, G. Csaba, L. Ji, A. Orlov, G. H. Bernstein, and W. Porod, Science **311**, 205 (2006).
[87] R. Richter, L. Bär, J. Wecker, and G. Reiss, Appl. Phys. Lett. **80**, 1291 (2002).